MALAYSIAN JOURNAL OF MICROSCOPY

Journal homepage: https://malaysianjournalofmicroscopy.org

RESEARCH ARTICLE

MORPHOLOGICAL AND STRUCTURAL STUDIES OF IRON OXIDE-CNT NANOCOMPOSITES BY ROBUST OXIDATION

Syahriza Ismail[1,*], Daniel Qayyum Anton[1], Noor Irinah Omar[2], Monna Rozanna[3]

[1]Faculty of Industrial and Manufacturing Technology and Engineering, Universiti Teknikal Malaysia Melaka, Hang Tuah Jaya, 76100 Durian Tunggal, Melaka, Malaysia.
[2]Faculty of Mechanical Technology and Engineering, Universiti Teknikal Malaysia Melaka, Hang Tuah Jaya, 76100 Durian Tunggal, Melaka, Malaysia.
[3]Research Center for Environmental and Clean Technology, National Research and Innovation Agency Republic of Indonesia, KST Samaun Samadikun, Bandung 40135, Indonesia.

Abstract. Heavy metals in wastewater pose a significant risk to the environment and human health due to their aquatic toxicity. This study investigates the optimal temperature for thermal oxidation to produce iron oxide nanowires and examines the adsorption capabilities of iron oxide-CNT (carbon nanotube) nanocomposites for heavy metal ions removal. Iron oxide nanowires facilitate magnetic separation post-adsorption, while CNTs provide a large surface area for the metal ion attraction. The iron oxide nanowires are synthesized through thermal oxidation, and the nanocomposite is formed via spin coating. Morphological and structural properties are analysed using Field Emission Scanning Electron Microscopy (FESEM), X-ray Diffraction (XRD), and Raman spectroscopy. The morphological studies show that the formation and properties of iron oxide nanowires can significantly vary with oxidation temperature. Temperatures between 450 °C and 650 °C have shown to produce a different crystalline peaks and morphologies. Thus, indicate that the formation and quantity of iron oxide nanostructures may vary with temperature. Meanwhile, adsorption capabilities of lead ions are assessed with UV-Vis spectroscopy by measuring the absorbance of heavy metal ions at specific wavelengths. With usage of the iron oxide- CNT nanocomposite, the absorption of the lead ions increases with longer immersion times. Thus, the iron oxide-CNT nanocomposites produced in this study has high potential for applications in wastewater treatment.

Keywords: Iron oxide, carbon nanotubes, oxidation.

Article Info

Received 6 January 2025
Accepted 9 October 2025
Published 4 December 2025

***Corresponding author: syahriza@utem.edu.my**

ISSN: 1823-7010, eISSN: 2600-7444

1. INTRODUCTION

Water pollution caused by heavy metals poses a significant environmental and public health challenge worldwide. These pollutants originate from industrial processes, urbanization, mining, and agriculture, leading to the contamination of critical water sources [1,2]. Owing to their non-degradable nature and acute or chronic toxicity, heavy metals such as lead, zinc, mercury, nickel, cadmium, copper, chromium, and arsenic threaten aquatic ecosystems and human health [3,4].

The rising concentration of heavy metals in wastewater necessitates removal technologies that are efficient, selective, and environmentally gentle [5,6]. Conventional treatment methods often suffer from limited adsorption capacity, poor selectivity, regeneration challenges, and secondary pollution. Nanocomposites that combine iron oxides with carbon nanotubes (CNTs) are promising due to the high surface area, tunable surface chemistry of CNTs, and the magnetic separability of iron oxides, which simplifies post-treatment recovery. However, iron oxide nanowire synthesis via thermal oxidation is highly sensitive to process parameters (temperature, time, ambient), which govern phase composition, defect density, and magnetic response. Despite prior studies on iron oxide formation, a systematic investigation isolating the role of oxidation temperature in controlling nanowire growth and resultant magnetic properties remains insufficiently resolved [7]. Works by Sahu and Queradhi [8], explores the various synthesis techniques including hydrothermal, sol–gel, and thermal decomposition. The role of temperature and synthesis conditions in controlling nanowire morphology and phase were discussed as well as the integration of iron oxide nanostructures with CNTs and their environmental application. Additionally, it was established that magnetic iron oxide nanocomposites exhibited the ability to attract heavy metals to their surface by electrostatic interactions, resulting in the elimination of the heavy metals ions from the liquid phase [9]. This was proven when α-Fe_2O_3 nanowires through oxidation has producing large-surface-area adsorbents to enable the simple removal of Cr ions from aqueous systems [10].

The objective of this work is to synthesized iron oxide nanowires with controlled morphology at optimized oxidation temperatures and demonstrated improved heavy metal adsorption efficiency of iron oxide-CNT nanocomposites relative to conventional adsorbents. In here the iron oxide nanowires were synthesized via thermal oxidation of iron foil, with variation of oxidation temperature to modulate nanowire nucleation, growth kinetics, and phase transformation. The structural, morphological, and magnetic characteristics of the nanowires were analysed to explain the correlation between oxidation temperature and material properties. Optimized nanowires were subsequently integrated with carbon nanotubes (CNTs) to fabricate a magnetically retrievable adsorbent, designed for heavy metal removal from wastewater. The central hypothesis suggests that precise control of oxidation temperature enhances nanowire crystallinity and magnetic responsiveness, thereby improving adsorption capacity and enabling efficient magnetic separation when coupled with CNTs. Characterization techniques included microscopy (FESEM) for morphological assessment, X-ray diffraction (XRD) for phase identification, and batch adsorption experiments to quantify remediation performance.

This study presents a systematic investigation of iron oxide nanowire growth through thermal oxidation, focusing on how temperature influences their shape and magnetic properties. It also demonstrates how these nanowires can be effectively combined with carbon nanotubes (CNTs) to create a magnetically separable material for removing heavy metals from wastewater. Unlike previous approaches, this work identifies temperature as a key factor in controlling nanowire quality and translates that understanding into a scalable composite with enhanced adsorption and easy recovery. Overall, it offers a practical framework linking synthesis conditions to material performance for environmental nanotechnology applications.

This project presents the synthesis of iron oxide nanowires across a temperature difference, characterizes their structural and magnetic properties, and evaluates the performance of CNT-integrated nanocomposites for adsorption and magnetic separation. The findings highlight implications for scalable wastewater treatment.

2. MATERIALS AND METHODS

2.1 Formation of Iron Oxide Nanowires by Thermal Oxidation

In this study, the iron foil was used as the substrate. The foil was cut into dimension of 1 cm × 2 cm and cleaned using three types of cleaning agents. First, the iron foil was immersed in a beaker containing 10 ml of ethanol solution and placed in an ultrasonic bath for 15 minutes. Then, the beaker was removed from the ultrasonic bath, and the iron foil was taken out and pat dried with tissue. Next, the iron foil cleaning process was repeated using acetone solution for another 15 minutes and finally, using 10 ml of distilled water for 10 minutes. Afterwards, the iron foil was dried using an air blower. Thermal oxidation process was chosen to form nanostructures on the iron foil surface. The iron foil was placed in an alumina boat, which was then positioned in the centre of the furnace. Thermal oxidation process was conducted at temperatures of 450 °C, 550 °C, and 650 °C for 2 hours. The process was carried out in ambient air with a heating rate of 10°C/min. After oxidation process is completed, the iron foil was left to cool in the furnace for 24 hours. Field emission scanning electron microscopy (FESEM) was use to analyse the morphology of the sample and X-ray diffraction (XRD) and Raman spectroscopy was employed to determine the crystalline nature of the iron oxide nanowires. A CuKα wavelength of 1.54 Å was used to determine the diffraction angle within the range of 20° to 90° (2θ).

2.2 Formation of Iron Oxide- CNT Nanocomposite by Robust Oxidation

Spin coating process was conducted after the iron oxide nanowires was formed. A volume of 10 ml of dimethylformamide (DMF) was added into the 100 ml beaker. Then, 0.25 g CNT powder was added in the beaker that containing DMF to make a CNT/DMF solution. This followed by sonification process using ultrasonic bath for 30 minutes. After 30 minutes of sonification, the CNT/DMF solution was ready to be used in spin coating process. The iron oxide nanowire was mounted on the spin coater chuck and correctly positioned it within the spin coating machine. After that, the CNT/DMF solution was poured onto the iron oxide nanowire surface. The step was repeated for another four times to complete a set of five layers of coating process. The parameters of this spin coating process were set at 3500 rpm of rotating speed and the spinning time was set to 120 s in order to get a uniform coating. The centrifugal force exerted during the spin coating process facilitates the spreading of the CNT/DMF solution onto the surface of iron oxide nanowire, resulting in the formation of iron oxide-CNT nanowires as the solvent evaporates. Similar characterization method using FESEM and XRD was employ to analyse the morphology and crystalline nature of the iron oxide-CNT nanocomposites.

2.3 Adsorption Test

The lead nitrate, $Pb(NO_3)_2$ stock solution was prepared by weighing a 1.6 g of Pb $(NO_3)_2$ using the weighing scale. Then the distilled water was filled into the 1000 ml volumetric flask until it was approximately half full. The measured 1.6 g of $Pb(NO_3)_2$ was added to the volumetric flask and then shaken to dissolve the $Pb(NO_3)_2$. The adsorption test of the iron oxide-CNT nanocomposites was performed using the prepared stock solution. In order to maintain the accuracy during the experiment, all glassware used was washed with nitric acid. During the adsorption test 100 ml of the stock solution was added to a beaker, and the pH level was examined using litmus paper. The pH of the stock solution was adjusted to 6 using either by using nitric acid or sodium hydroxide. Next, a piece of α-Fe_2O_3-CNT was soaked in the solution for 30 minutes. After 30 minutes, the α-Fe_2O_3-CNT was removed from the beaker. This experiment was repeated with different immersion times of 60, 90, and 120 minutes. Finally, the concentration of Pb(II) ions in the stock solution was determined using UV-visible spectroscopy.

3. RESULTS AND DISCUSSION

3.1 Morphological Analysis

FESEM images of the iron foil that has been oxidized for 2 hours in furnace at 450 °C, 550 °C and 650 °C are presented in Figure 1. It was observed that at oxidation temperature of 450 °C, the iron oxide nanostructure is in the form of nanoleaf. At 550 °C and 650 °C the nanoleaf structures has transform into nanowires Most nanowires in Figure 1(b)ii and (c)ii span approximately 1 to 3 µm in length. Some longer wires may slightly exceed 3 µm, but the majority fall within this range. Whereas the diameter is estimated to be between ~50 nm and 150 nm. However, the quantity of nanowires in both temperatures are varied. The distribution of nanowires formed at 550 °C are higher compared to 650 °C oxidation temperature. This concluded that that the oxidation temperatures may have a significant influence of the structure formation possible due to the different stress exposed to the iron foil during the process [11].

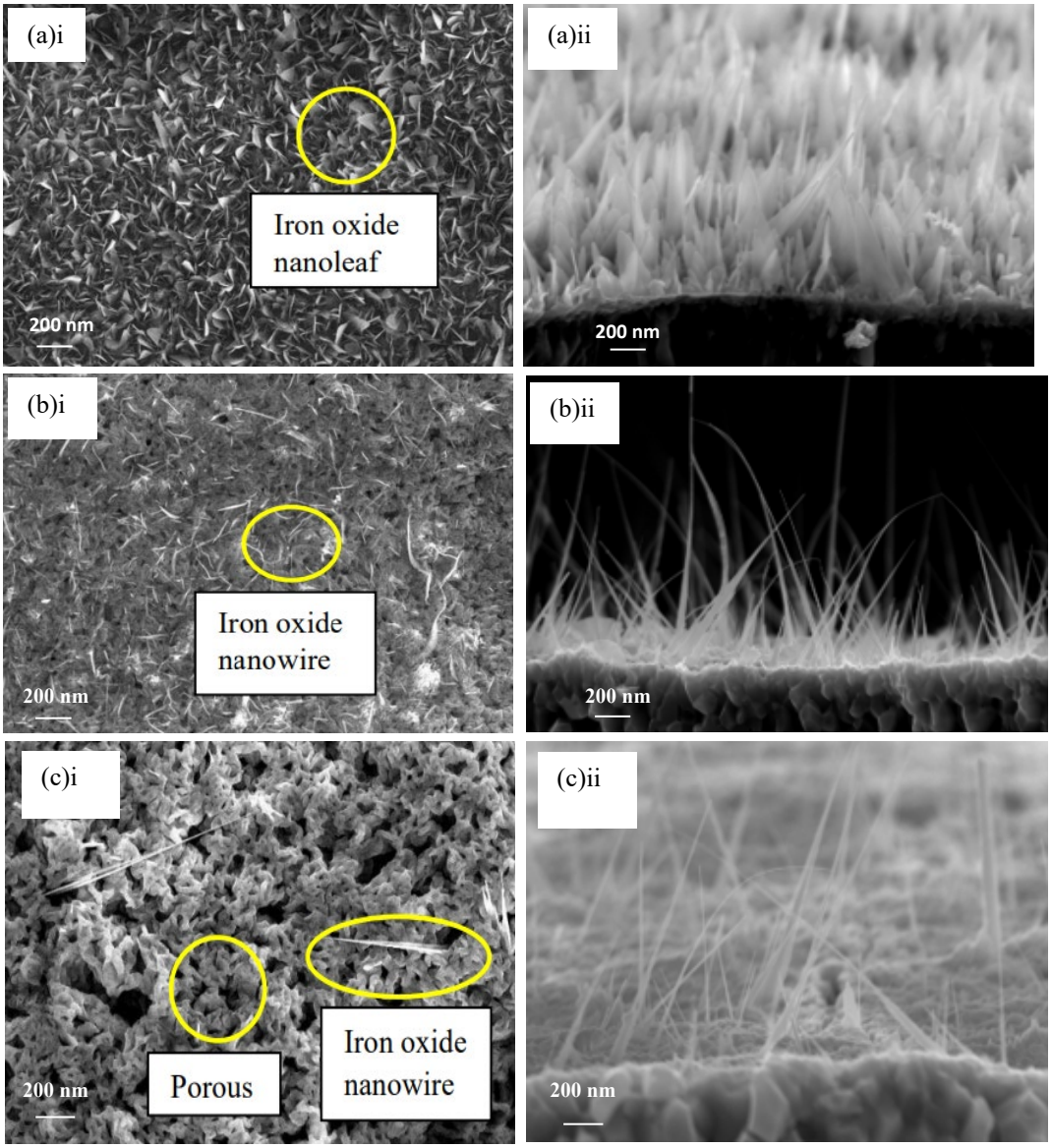

Figure 1: FESEM images of iron oxide nanostructure at different temperature top view: (a-i) 450 °C, (b-i) 550 °C, (c-i) 650 °C and side view (a-ii) 450 °C, (b-ii) 550 °C, (c-ii) 650 °C

When iron foil is exposed to varying temperatures during oxidation or nanostructure growth, it experiences different types of thermal and mechanical stresses, which significantly influence the resulting surface morphology. At higher temperatures, the material undergoes thermal expansion, which can introduce compressive or tensile stress depending on the temperature gradient and the oxide layer formation. These stresses arise from the mismatch in thermal expansion coefficients between the iron substrate and the growing oxide layer (Fe_2O_3), leading to strain accumulation at the interface. Additionally, growth stress occurs during the formation of nanostructures or oxide layers, especially when atoms rearrange or migrate rapidly at elevated temperatures. This can cause grain boundary movement, dislocation generation, and surface roughening, resulting in different morphologies such as porous structures, cracks, or coarser grains.

At the same time, it was observed that the pores size and area formed at 650 °C is larger, possibly due to higher oxidation rate thus producing coarser nanostructure and thicker oxide layer. At elevated temperatures such as 650 °C, the oxidation process accelerates due to increased reaction kinetics and enhanced atomic mobility, allowing oxygen to diffuse more rapidly into the material. This leads to the formation of a thicker oxide layer and promotes coarser nanostructure growth, as atoms have more energy to migrate and reorganize. The rapid oxidation also induces stress and volume expansion, which can result in pore formation and increased surface roughness. Consequently, the porous area becomes larger, reflecting the combined effects of faster oxidation, thicker oxide formation, and coarser structural development at higher temperatures. Hence, the sample oxidized at 550 °C was choose for the nanocomposite formation because of the high distribution and amount of nanowires growth.

FESEM images in Figure 2 show the morphological of α-Fe_2O_3-CNT after the spin coating. The formation of α-Fe_2O_3-CNT nanocomposite was successfully produced with the MWCNTs structured appeared to be entangled in between the iron oxide nanowires. The formation of iron oxide-CNT nanocomposite looks compact because of the MWCNTs covering all the space between the iron oxide nanowires. Figure 2(a) show the present of iron oxide nanowires as well as MWCNTs which is in the form of flakes can be observed. This finding suggests that the thickness of the MWCNTs is not too thick to cover the iron oxide nanowires. At higher magnification (Figure 2(b)), confirms the present of MWCNT in the sample. The increasing of magnification value provides more detailed and closer view of the MWCNTs.

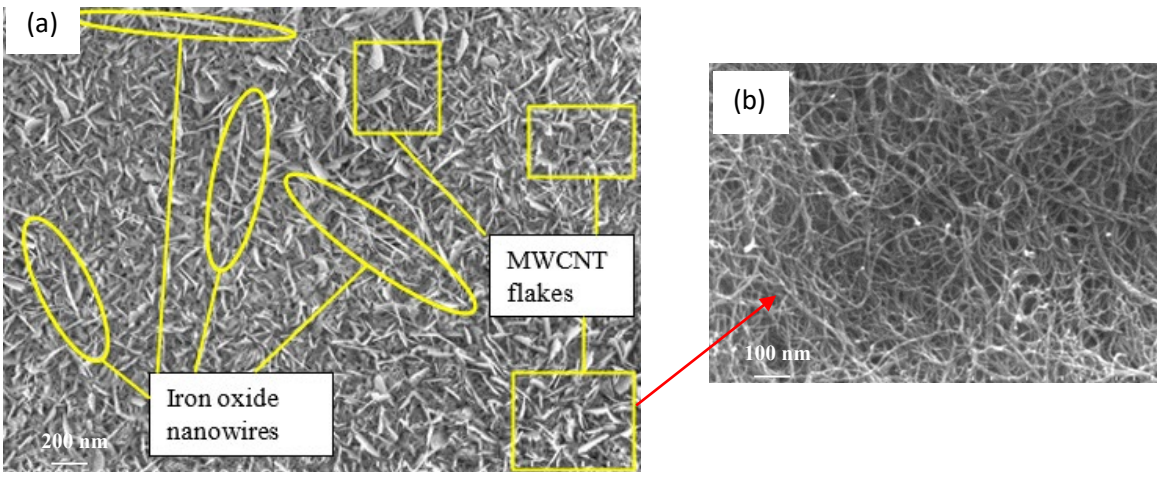

Figure 2: FESEM images (top view) of α-Fe_2O_3-CNT at different magnifications (a)10k and (b) 50k

3.2 Structural Analysis

The structural analysis was analysed by using XRD and Raman spectroscopy. Figure 3 shows the XRD pattern of iron oxide nanostructure oxidize in different temperatures respectively. Based on the peaks of XRD obtained, the nanostructure is suggested to be in hematite phase. The peaks at 2θ are approximately 24.18°, 33.13°, 35.57°, 40.93°, 49.43° and 54.13° which is corresponding to 012, 104, 110, 113, 024 and 116 planes. These peaks are match with previous study of α-Fe_2O_3 phase [12]. For bulk structures, the stable temperature for hematite is 500-550 °C. However, under controlled thermal oxidation (e.g., in air or oxygen-rich environments), hematite nanowires can nucleate and grow via stress-induced grain boundary diffusion and anisotropic crystal growth. This can favour the formation of thermodynamically stable hematite even at slightly lower temperatures.

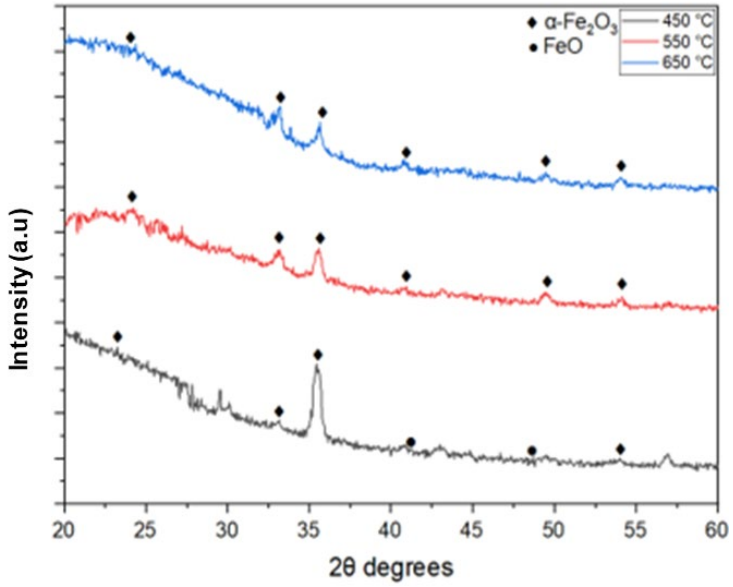

Figure 3: XRD patterns of iron oxide nanostructure oxidize at 450, 550 and 650 °C

Figure 4 shows the Raman spectra of iron oxide nanostructure oxidize in different temperatures respectively. The peaks value obtained in this study is approximately 225.71, 244.92, 291.70, 409.52 and 613.57 cm^{-1}. These peaks also similar with previous study that confirmed the present of α-Fe_2O_3 [12].

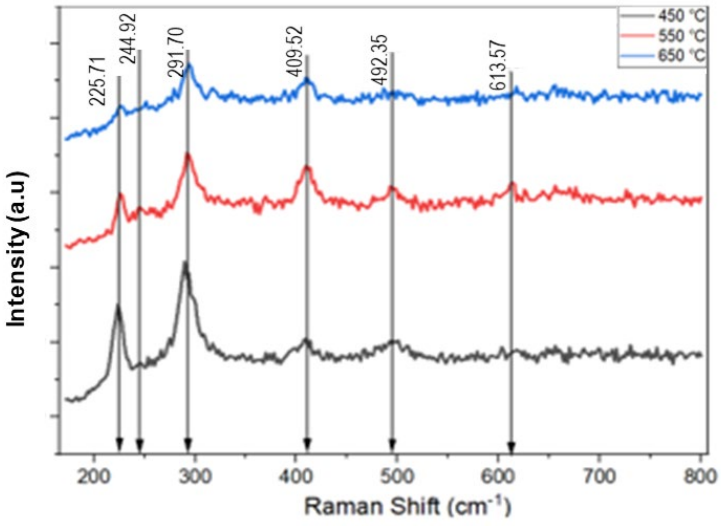

Figure 4: Raman spectra of iron oxide nanostructure oxidize at 450, 550 and 650 °C

Figures 5 shows the XRD pattern of α-Fe_2O_3-CNT nanocomposites respectively. The peaks of XRD are identical with the XRD peaks in Figure 3. However, the MWCNTs peaks are at 23.98° and 43.08°which is corresponding to 002 and 100 planes. These peaks are match with previous study that exhibits the peaks of both α-Fe_2O_3 and MWCNTs [13].

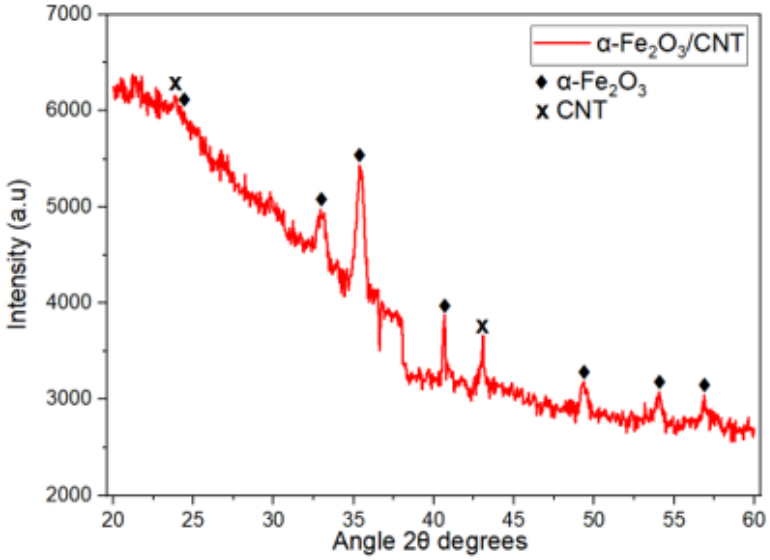

Figure 5: XRD pattern of α-Fe_2O_3-CNT nanocomposite

While for Raman spectra, as shown in Figure 6, the present of peak at 100 to 700 cm^{-1} and 1324.90 cm^{-1} are consistent with typical α-Fe_2O_3 phase. The D-band is 1341.50 cm^{-1} while the G- band is 1580.50 cm^{-1} are similar as reported by previous study [14], indicates D-band and G-band peaks that corresponding to the present of MWCNTs. The presence of multiple RBM peaks; 261.64 cm^{-1}, 225.38 cm^{-1}, 316.79 cm^{-1} indicates a distribution of CNT. This confirms the structural integrity of CNTs in the iron oxide-CNT nanocomposites and supports the role in environmental applications.

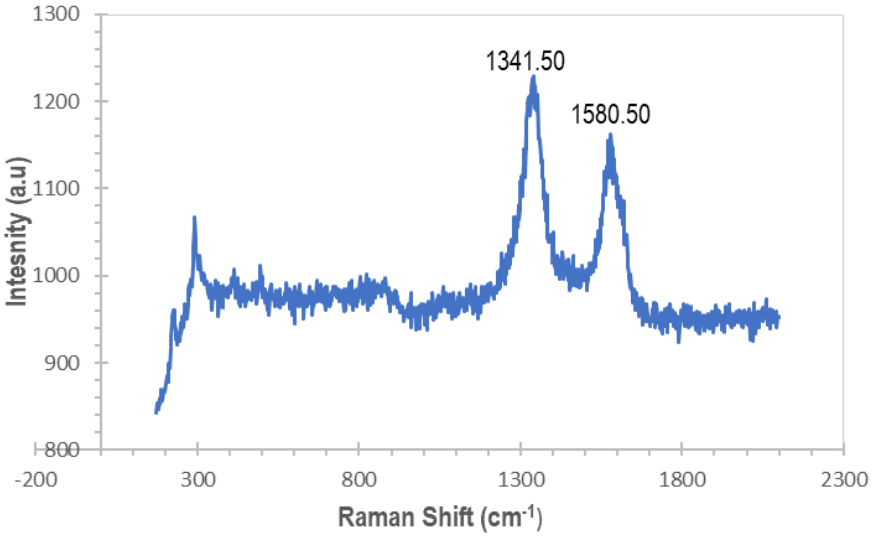

Figure 6: Raman spectra of α-Fe_2O_3-CNT nanocomposite

3.3 Adsorption Test

Figure 7 shows the plot of absorbance vs wavelength that obtained by UV- Vis Spectroscopy. From the graph, at 30 minutes immersion time, the absorbance peak is at the lowest while at 120 minutes

immersion time, the absorption peak is at the highest. These results show that as the immersion time increase, the absorbance peak also increase. From the graph, a qualitative comparison was made by extracting the absorbance values at 300 nm wavelength and presented in Table 1. At 300 nm, the absorbance values were 0.41, 0.72, 0.79, and 1.20 for immersion times of 30, 60, 90, and 120 minutes, respectively. The initial absorbance from 30 to 60 minutes suggests partial desorption or reorganization of surface-bound species. As the reaction period progresses to 90 minutes, a slight increase indicates gradual re-adsorption or stabilization of species on the surface. By 120 minutes, the absorbance rises significantly compared to 30 minutes, reflecting enhanced adsorption of species onto the material. This increase in surface coverage promotes stronger light–matter interaction, thereby improving the absorbance intensity. As the immersion time increase, the concentration of the stock solution is decrease. This is because the iron oxide-CNT nanocomposites adsorb the lead ions on the surface. This adsorption process highlights the potential of α-Fe_2O_3-CNT nanocomposites for effectively reducing heavy metal concentrations in contaminated water, providing a promising approach for wastewater treatment applications.

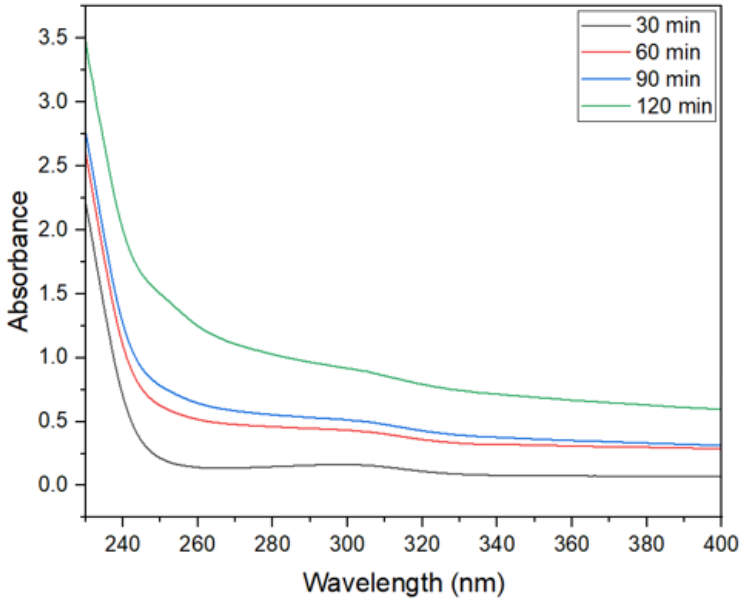

Figure 7: Absorbance at different time vs Wavelength graph

Table 1: Quantitative comparison based on the absorbance values extracted at 300 nm

Time (min)	Absorbance at 300 nm
30	0.41
60	0.72
90	0.79
120	1.20

4. CONCLUSIONS

This study successfully synthesized and characterized iron oxide nanowires via thermal oxidation, identifying that 550 °C as the optimal temperature for achieving well-defined morphology and enhanced crystallinity. Structural and morphological analyses using FESEM, XRD, and Raman spectroscopy confirmed the formation of phase-pure nanowires with temperature-dependent growth behaviour. Integration of these nanowires with carbon nanotubes (CNTs) resulted in a magnetically retrievable nanocomposite with high adsorption efficiency for heavy metal ions in wastewater. UV-Vis

spectroscopy revealed that adsorption capacity increased with immersion time, indicating strong interaction between the composite surface and metal ions. These findings demonstrate that temperature-controlled synthesis directly influences the nanowire's magnetic and structural properties, which in turn govern the composite's adsorption performance. Overall, this work provides a scientifically grounded framework for designing scalable, high-performance nanomaterials for environmental remediation, with potential applications in industrial wastewater treatment and resource recovery.

Acknowledgements

The authors gratefully acknowledge Universiti Teknikal Malaysia Melaka (UTeM) for the financial support and the Faculty of Industrial and Manufacturing Technology and Engineering, for providing the laboratory facilities.

Author Contributions

All authors contributed toward data analysis, drafting and critically revising the paper and agree to be accountable for all aspects of the work.

Disclosure of Conflict of Interest

The authors declare no potential conflict of interest in the publication of this work.

Compliance with Ethical Standards

The work is compliant with ethical standards

References

[1] Vidu, R., Matei, E., Predescu, A. M., Alhalaili, B., Pantilimon, C., Tarcea, C. & Predescu, C. (2020). Removal of heavy metals from wastewaters: A challenge from current treatment methods to nanotechnology applications. *Toxics,* 8(4), 101.

[2] Qasem, N. A. A, Mohammed, R. H. & Lawal, D. U. (2021). Removal of heavy metal ions from wastewater: A comprehensive and critical review. *Npj Clean Water,* 4(1), 36.

[3] Seffah, K., Zafour-Hadj-Ziane, A., Tarek, A. A., Guillet, J. F., Lonchambon, P. & Flahaut, E. (2017). Adsorption of cadmium ions from water on double-walled carbon nanotubes iron oxide composite. *Chemistry Journal of Moldova*, 12(2), 71-78.

[4] Ismanto, A., Hadibarata, T., Widada, S., Indrayanti, E., Ismunarti, D. H., Safinatunnajah, N., Kusumastuti, W., Dwiningsih. Y. & Alkahtani, J. (2023). Groundwater contamination status in Malaysia: level of heavy metal, source, health impact, and remediation technologies. *Bioprocess and Biosystems Engineering*, 46(3), 467-482.

[5] Briffa, J., Sinagra, E. & Blundell, R. (2020). Heavy metal pollution in the environment and their toxicological effects on humans. *Heliyon,* 6(9), e04691.

[6] Mitra, S., Chakraborty, A. J., Tareq, A. M., Emran, T. B., Nainu, F., Khusro, A., Idris A. M., Kandaker, M. U., Hamid, O., Alhumaydhi, F.A. & Simal-Gandara, J. (2022). Impact of heavy metals

on the environment and human health: Novel therapeutic insights to counter the toxicity. *Journal of King Saud University-Science*, 34(3), 101865.

[7] Aniołek, K., Barylski, A. & Kupka, M. (2018). Modelling the structure and mechanical properties of oxide layers obtained on biomedical Ti-6Al-7Nb alloy in the thermal oxidation process. *Vacuum,* 154, 309-314.

[8] Sahu, T. K. & Qureshi, M. (2024). Synthesis, Morphology and Environmental Applications of Iron Oxide-Based Nanoarchitectures. In *Iron Oxide-Based Nanocomposites and Nanoenzymes. Nanostructure Science and Technology.* Ed. Sahoo, H. & Sahoo, J. K. (Cham: Springer International Publishing), pp. 169-184.

[9] Mbuyazi, T. B. & Ajibade, P. A. (2024). Magnetic iron oxides nanocomposites: synthetic techniques and environmental applications for wastewater treatment. *Discover Nano,* 19, 158.

[10] Budiman, F., Tan, W. K., Kawamura, G., Muto, H., Matsuda, A., Abdul Razak, K. & Lockman, Z. (2021). Formation of dense and high-aspect-ratio iron oxide nanowires by water vapor-assisted thermal oxidation and their Cr (VI) adsorption properties. *ACS Omega*, 6(42), 28203-28214.

[11] Budiman, F., Bashirom, N., Tan, W. K., Razak, K. A., Matsuda, A. & Lockman, Z. (2016). Rapid nanosheets and nanowires formation by thermal oxidation of iron in water vapour and their applications as Cr (VI) adsorbent. *Applied Surface Science*, 380, 172-177.

[12] Ilmi, M. M., Nurdini, N., Maryanti, E., Setiawan, P. & Ismunandar, I. (2021). X-ray diffraction peak profile for determination of microstructural properties of hematite (Fe_2O_3). *Journal of Research and Development on Nanotechnology*, 1(1), 11-17.

[13] Banbela, H. M., Alharbi, L. M., Al-Dahiri, R. H., Jaremko, M. & Abdel Salam, M. (2022). Preparation, characterization, and electrochemical performance of the hematite/oxidized multi-walled carbon nanotubes nanocomposite. *Molecules,* 27(9), 2708.

[14] Oh, S. H., Kwon, O. H., Kang, Y. C., Kim, J. K. & Cho, J. S. (2019). Highly integrated and interconnected CNT hybrid nanofibers decorated with α-iron oxide as freestanding anodes for flexible lithium polymer batteries. *Journal of Materials Chemistry A*, 7(20), 12480-12488.